Chinese Journal of Electronics
vol. 33, no. 5, pp. 1218–1223, September 2024
https://doi.org/10.23919/cje.2023.00.033

RESEARCH ARTICLE

A Microstrip Leaky-Wave Antenna with Scanning Beams Horizontal to the Antenna Plane

Henghui WANG, Peiyao CHEN, and Sheng SUN

School of Electronic Science and Engineering, University of Electronic Science and Technology of China, Chengdu 611731, China

Corresponding author: Sheng SUN, Email: sunsheng@uestc.edu.cn
Manuscript Received February 6, 2023; Accepted October 27, 2023

Abstract — A leaky-wave antenna with horizontal scanning beams and broadside radiation is presented on the periodically modulated microstrip. The horizontal radiation is realized by periodically etching a set of resonant open-ended slots on the ground plane. Dispersion diagrams and Bloch impedance are first analyzed to investigate the propagation and radiation characteristics of the periodic structure. Subsequently, shunt matching stubs are installed aiming to obtain seamless beam scanning property through the broadside. Finally, a prototype is implemented as verification of the presented antenna. Results of the simulations and measurements agree well with each other, indicating the elimination of the open-stop band effect and the horizontal radiation beams. The fabricated antenna exhibits a beam range from −62° to +34°, and provides a maximum measured gain about 14.6 dBi at 10 GHz.
Keywords — Bloch impedance, Horizontal radiation, Leaky-wave antenna, Microstrip line, Seamless beam scanning.
Citation — Henghui WANG, Peiyao CHEN, and Sheng SUN, "A Microstrip Leaky-Wave Antenna with Scanning Beams Horizontal to the Antenna Plane," *Chinese Journal of Electronics*, vol. 33, no. 5, pp. 1218–1223, 2024. doi: 10.23919/cje.2023.00.033.

I. Introduction

Planar leaky-wave antennas (LWAs) have been extensively researched because of their merits of broad bandwidth [1]–[6], low profile, the beam-scanning property, and high gain [7], [8]. Unfortunately, gain of the LWA is degraded when working around the broadside frequency, which is called the open-stop band effect [9], [10]. To suppress this effect and realize seamless beam scanning with stable gain around the broadside direction, various methods have been researched and conducted [11]–[20], including adding extra matching stubs [11], pins [15], or slots [20], using the phase-reversal method [12], and introducing additional transversal asymmetry [13], [14]. The composite right/left handed (CRLH) structure is also effective candidate for open-stop band suppression [21]–[25].

Most of the reported periodic LWAs provide vertical radiation beams [26]–[31]. Compared with the conventional vertical beams, the horizontal beams are more attractive because of the narrower radiation aperture. The radiation aperture of vertically radiating LWA is usually along the upper surface of the circuit board, while the aperture of the horizontally radiating LWA is along the side wall of the circuit board. Therefore, the horizontally radiating antenna has the merit of a smaller radiation aperture and can be used in narrower spaces. Meanwhile, the vertically radiating antenna must be on the outermost layer of the multilayer circuit board, while the horizontally radiating antenna can be located inside the multilayer circuit board, and then the circuit board can be shielded on both sides to prevent electromagnetic interference. However, LWAs with horizontal radiation beams have been rarely investigated during the last decades [32]–[35]. An LWA with horizontal beams was presented in [32] based on an asymmetric CRLH coplanar strips (CPS) structure. References [33] and [34] present horizontally radiating LWAs by loading a pair of branches on both surfaces of the substrate integrated waveguide (SIW). In [35], the horizontal radiation can also be realized by introducing asymmetric periodical modulation on the spoof surface plasmon polariton (SSPP) structure. However, the reported horizontally ra-

Associate Editor: Prof. Yinghong WEN, Beijing Jiaotong University.

diating LWAs still suffer from the complicated structure, the limited gain, or the narrow scanning range.

The Vivaldi antenna, as shown in Figure 1(a), features the end-fire radiation beam parallel to the antenna plane [36], [37]. By combining the theory of Vivaldi antenna and the design method of traditional periodic LWA, a horizontally radiating LWA is proposed based on a microstrip-fed periodic structure. Inspired by the physical mechanism of Vivaldi antenna, two different LWA unit cells are first analyzed and discussed. To interpret the propagation and radiation characteristics of the proposed periodic structure, propagation constants and Bloch impedance are studied based on the full-wave simulation software. Then, open-ended stubs are further amounted along the microstrip line (MSL) to balance the Bloch impedance, thus suppressing the gain degradation at the broadside frequency. Finally, a design prototype with 20 cells is developed and implemented. The simulated broadside radiation and horizontal beam scanning performance are experimentally validated by measured results.

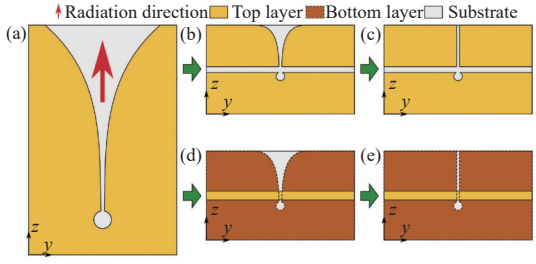

Figure 1 Structures of (a) The conventional Vivaldi antenna, (b) CPS-fed Vivaldi-like unit, (c) CPS-fed rectangular-slot unit, (d) MSL-fed Vivaldi-like unit, and (e) MSL-fed rectangular-slot unit.

II. Working Principle and Unit Analysis

1. Radiation mechanism

Figures 1(b) and (d) show the structures of the presented Vivaldi-like LWA periodic unit fed by the CPS and MSL, respectively. In the unit, the tapered open-ended slot is excited by the transmission line and leaks energy to the horizontal direction through the slot. A circular area is etched on the other end of the slot to balance the mode conversation impedance of the slot excitation. Therefore, the radiation direction of the designed unit is along the z-axis, i.e., the horizontal direction along the circuit board plane. However, the exponentially tapered slot causes large attenuation constant at frequencies far away from the broadside frequency, which is detrimental to the wide-angle scanning range. Thus, the improved units are presented as shown in Figures 1(c) and (e), in which the exponentially tapered slot is replaced by the rectangular open-ended slot.

In this design, the MSL-fed rectangular-slot unit is adopted for the realization of horizontal radiation. The transmission mode of the MSL is the EH_0-mode, and the etched rectangular-slot is equivalent to a slot-line and uses the slot-line-mode for radiation. Figures 2(a) and (b) show the geometry and its equivalent model. Compared with the CPS-fed unit, the MSL-fed unit has several advantages. Firstly, the CPS-fed unit needs a mode converter to excite the CPS mode while the MSL-fed unit can be easily fed by the microstrip transmission line. Secondly, the MSL-fed unit is easier to realize a Bloch impedance of 50 Ω than the CPS-fed unit. Thus, there is no need of additional impedance transformer. Thirdly, a strong CPS mode will be excited in the rectangular slot of the CPS-fed unit, which causes undesired radiation beams in the vertical direction. In the transversal direction of the MSL-fed unit, the microstrip mode is the primary mode near the host transmission line. Therefore, the CPS mode on the rectangular slot is weakened and the vertical radiation component can be effectively suppressed.

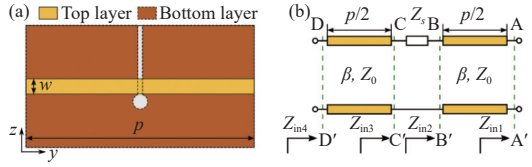

Figure 2 (a) Configuration of the initial LWA unit. (b) Equivalent circuit.

2. LWA unit design and open-stop band suppression

According to the frequency balanced condition [10], the open-ended slot is utilized and designed for the elimination of the open-stop band at first. Figure 3 shows the Bloch impedance based on different MSL characteristic impedance. Similar to [20], the resultant Bloch impedance Z_B becomes higher than the characteristic impedance Z_0. Meanwhile, it is shown that Bloch impedances reach extremum values at 10 GHz, revealing the severe open-stop band effect.

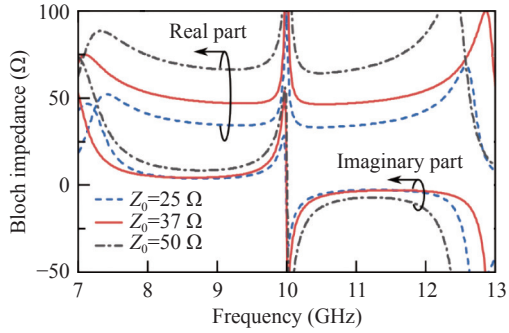

Figure 3 Investigations of the Bloch impedance.

As shown in Figure 2(b), at the right side of AA′ plane, the impedance is assumed as Z_{in1}. Then, the input impedances before and after the rectangular slot are Z_{in2} and Z_{in2}, respectively. Z_{in4} represents the input impedance after whole periodic unit. At the broadside frequency, the unit length p is about a guided-wave-

length. Thus, Z_{in2} and Z_{in4} can be expressed as follows:

$$Z_{in2} = Z_{in1} \tag{1}$$

$$Z_{in4} = Z_{in3} \tag{2}$$

Meanwhile, the loaded slot can be equivalent to a series radiation resistance at this frequency. Assuming the radiation resistance as R_s, Z_{in3} is obtained as

$$Z_{in3} = Z_{in2} + R_s \tag{3}$$

Substitute (1) and (2) into (3), the input impedance after one periodic unit is expressed as

$$Z_{in4} = Z_{in1} + R_s \tag{4}$$

Notice that the input impedance increases by R_s after each periodic unit. Therefore, the input impedance of the periodic structure keeps increasing as the number of cascaded units increases, which is corresponding to the drastic variation on the Bloch impedance. Therefore, a pair of shunt open-ended stubs are installed to the unit cell to balance the Bloch impedance, as the configuration and equivalent circuit model are shown in Figure 4. The shunt stubs introduce the shunt capacitive admittance Y_m and compensate the inductive effect of the input admittance. Hence, the resultant reflection coefficient becomes smaller and the Bloch impedance can thus be effectively matched.

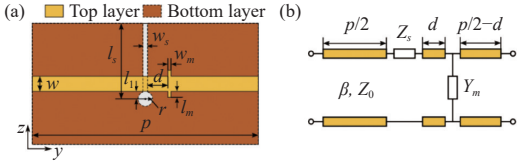

Figure 4 (a) Configuration of the matched LWA unit. (b) Equivalent circuit.

Based on the ABCD matrix extracted by the full-wave method of the unit, the propagation constant γ_u and Bloch impedance Z_B are calculated as follows:

$$\gamma_u = \alpha_u + \mathrm{j}\beta_u = \frac{1}{p}\mathrm{arccosh}\left(\frac{A+D}{2}\right) \tag{5}$$

$$Z_B^{\pm} = \frac{-2B}{2A - A - D \mp \sqrt{(A+D)^2 - 4}} \tag{6}$$

where α_u is the leakage constant and β_u is the phase constant.

Details of the dispersion behavior and the Bloch impedance are shown in Figure 5. Due to the loaded matching stubs, the normalized attenuation constant and the Bloch impedance are balanced, revealing the eliminated open-stop band effect.

To further reduce the backlobe of the LWA, the ground plane is widened on the opposite side of the rectangular open-ended slot. By considering the coupling effect of the series units, the final dimensions of the fabricated LWA are tabulated in Table 1.

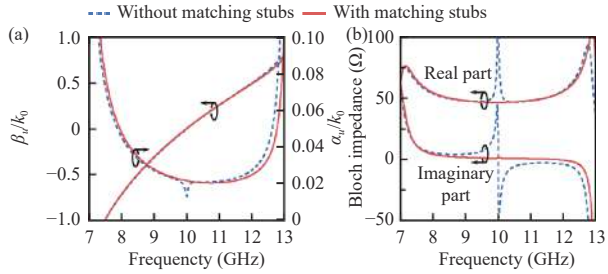

Figure 5 (a) Dispersion diagrams and (b) Bloch impedance of the periodic units.

Table 1 Dimensional parameter of the fabricated LWA (unit: mm)

Parameters	Value	Parameters	Value	Parameters	Value
p	13.7	w	1.5	d	1.75
r	1.0	w_s	0.2	w_m	0.3
l_1	0.75	l_s	3.6	l_m	0.32

III. LWA Design and Measurement

To verify the performance of the presented antenna, an LWA containing 20 units is designed and fabricated. The substrate is Rogers 3006 and thickness is 0.635 mm ($\varepsilon_r = 6.15$, $\tan\delta = 0.0025$). To avoid the additional impedance transformer at the two ends of the LWA, the Bloch impedance is designed as about 50 Ω, and the corresponding transmission line characteristic impedance is about 37 Ω. The photograph of the antenna is shown in Figure 6, which is fed by End Launch connecters through a pair of MSL with characteristic impedance of 50 Ω.

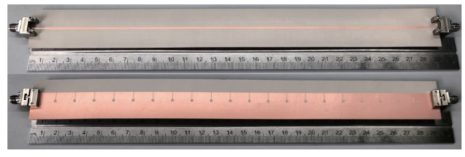

Figure 6 Antenna photograph.

The simulated $|S_{11}|$ and $|S_{21}|$ together with the measurements are shown in Figure 7. A small frequency shift exists mainly due to the tolerance of the relative permittivity ε_r. By correcting the relative permittivity as 6.7, the simulations and the measurements agree with each other. Notice that due to the modified relative permittivity, a slight degradation on $|S_{11}|$ at the measured broadside frequency 9.65 GHz is observed. The measured $|S_{21}|$ is lower than –10 dB in the whole working band, revealing that at least 90% of the input power is consumed by the LWA. Figure 8 shows the realized gain and the corresponding radiation directions, and the radiation efficiency is shown in Figure 9. The measurements are accordant with the modified simulations, showing a gain variation of 9.6 dBi to 14.6 dBi. In the working frequency band of 7.5 GHz to 11.6 GHz, the amplitude of the

transmission coefficient decreases with the decreasing frequency, meaning that the lower working frequency radiates more energy. Therefore, the radiation efficiency increases as the frequency decreases. When the frequency is greater than 11.6 GHz, there is a significant increase in radiation efficiency. However, this frequency band is the stopband, and the directivity of the LWA is very small, so the antenna gain decreases obviously when frequency exceeds 11.6 GHz. Due to the conductor loss and the dielectric loss, the final average radiation efficiency in the working band is about 75%.

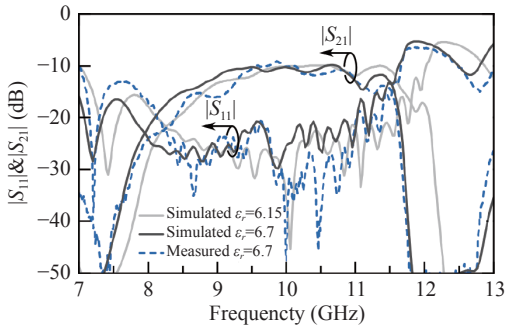

Figure 7 Results of transmission coefficient and reflection coefficient with original and modified relative permittivity.

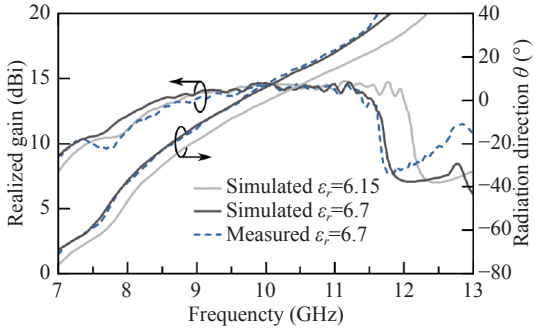

Figure 8 Realized gain and beam angle with original and modified relative permittivity.

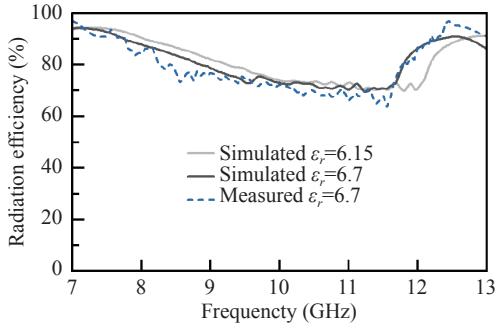

Figure 9 Results of efficiency.

The simulated 3-D pattern at the broadside frequency is depicted in Figure 10 with the horizontally radiating main beam. Result of the H-plane pattern are given in Figure 11, showing agreement with the simulated result.

Figure 12 shows E-plane patterns at several beam

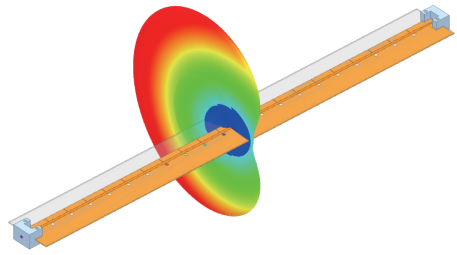

Figure 10 Simulated 3-D pattern at 10 GHz.

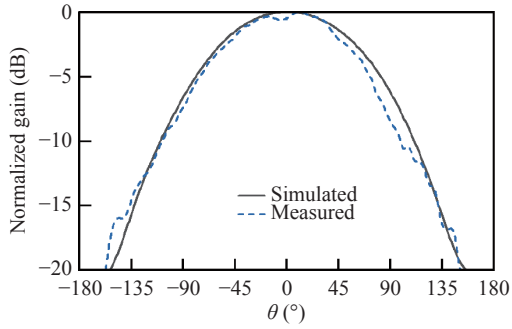

Figure 11 H-plane radiation patterns at the broadside frequency.

angles. The beam angle of the LWA is related to the working frequency, and therefore, the frequency shift causes that the measured frequency is slightly smaller than the simulated at the same beam angle. The main beam scans from −62° to +34° in the simulated band of 7.6 GHz to 12.1 GHz and in the measured band of 7.5 GHz to 11.6 GHz. The antenna scans from −35° to +34° when the gain variation is lower than 3 dB. Due to the reduction of the radiation aperture with the decreased frequency, the beamwidth of the radiation patterns get broad at low frequencies.

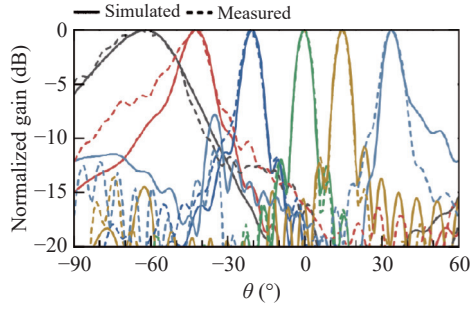

Figure 12 E-plane radiation patterns at several beam angles. Curves with different color represent various operating frequencies in GHz: Black 7.5–7.6; Red 7.85–8.1; Dark blue 8.6–8.9; Green 9.65–10.0; Yellow 10.55–11; Blue 11.6–12.1.

Comparison between the presented LWA and several reported LWAs is tabulated in Table 2. The configuration of the proposed LWA is simplified compared with [32]–[34], and the designed LWA exhibits the excellent performance of horizontal radiation and wide-angle beam scanning property through broadside. Compared with [32], the normalized attenuation constant of the proposed antenna is reduced, and therefore, gain of the proposed LWA is

greatly improved by increasing the antenna length.

Table 2 Comparison between designed antenna and reported literature

Structure	Radiation direction	Maximum gain (dBi)	Total length ($\times\lambda_0$)	Scanning range (°)
MSL [16]	Vertical	14	7.2	−48 to 35
CPS [12]	Vertical	16	15	−76 to 40
CPS [32]	Horizontal	7.4	1.3	−79 to 56
SIW [33]	Horizontal	12.0	8.1	−43 to 43
SIW [34]	Horizontal	10.5	6.5	−49 to 58
SSPP [35]	Horizontal	13.7	16.9	−10 to 8
This work MSL	Horizontal	14.6	9.8	−62 to 34

IV. Conclusion

A horizontally radiating LWA with broadside radiation has been analyzed and designed in this work. Rectangular open-ended slots are etched on the ground plane of the microstrip structure to provide horizontal radiations. The LWA can be applied in wireless communication systems under narrow space, with the 10-dB reflection coefficient bandwidth covering the X-band. The designed antenna scans from −62° to +34° with measured gain variation of 9.6 dBi to 14.6 dBi. Results of both the simulations and the measurements confirm the antenna merit of seamless horizontal scanning beams.

Acknowledgements

This work was supported by the National Natural Science Foundation of China (Grant Nos. 61971115 and 61721001), and the Sichuan Science and Technology Program (Grant No. 2023NSFSC0486).

References

[1] J. T. Williams, P. Baccarelli, S. Paulotto, *et al.*, "1-D combline leaky-wave antenna with the open-stopband suppressed: Design considerations and comparisons with measurements," *IEEE Transactions on Antennas and Propagation*, vol. 61, no. 9, pp. 4484–4492, 2013.

[2] Y. L. Lyu, X. X. Liu, P. Y. Wang, *et al.*, "Leaky-wave antennas based on noncutoff substrate integrated waveguide supporting beam scanning from backward to forward," *IEEE Transactions on Antennas and Propagation*, vol. 64, no. 6, pp. 2155–2164, 2016.

[3] A. Kianinejad, Z. N. Chen, and C. W. Qiu, "A single-layered spoof-plasmon-mode leaky wave antenna with consistent gain," *IEEE Transactions on Antennas and Propagation*, vol. 65, no. 2, pp. 681–687, 2017.

[4] K. Rudramuni, K. Kandasamy, Q. F. Zhang, *et al.*, "Goubauline leaky-wave antenna for wide-angle beam scanning from backfire to endfire," *IEEE Antennas and Wireless Propagation Letters*, vol. 17, no. 8, pp. 1571–1574, 2018.

[5] Y. L. Lyu, F. Y. Meng, G. H. Yang, *et al.*, "Periodic leaky-wave antenna based on complementary pair of radiation elements," *IEEE Transactions on Antennas and Propagation*, vol. 66, no. 9, pp. 4503–4515, 2018.

[6] R. Ranjan and J. Ghosh, "SIW-based leaky-wave antenna supporting wide range of beam scanning through broadside," *IEEE Antennas and Wireless Propagation Letters*, vol. 18, no. 4, pp. 606–610, 2019.

[7] A. Sarkar, D. A. Pham, and S. Lim, "Tunable higher order mode-based dual-beam CRLH microstrip leaky-wave antenna for V-band backward-broadside-forward radiation coverage," *IEEE Transactions on Antennas and Propagation*, vol. 68, no. 10, pp. 6912–6922, 2020.

[8] A. Sarkar, A. H. Naqvi, and S. Lim, "(40 to 65) GHz higher order mode microstrip-based dual band dual beam tunable leaky-wave antenna for millimeter wave applications," *IEEE Transactions on Antennas and Propagation*, vol. 68, no. 11, pp. 7255–7265, 2020.

[9] S. Rezaee and M. Memarian, "Analytical study of open-stopband suppression in leaky-wave antennas," *IEEE Antennas and Wireless Propagation Letters*, vol. 19, no. 2, pp. 363–367, 2020.

[10] S. Otto, A. Rennings, K. Solbach, *et al.*, "Transmission line modeling and asymptotic formulas for periodic leaky-wave antennas scanning through broadside," *IEEE Transactions on Antennas and Propagation*, vol. 59, no. 10, pp. 3695–3709, 2011.

[11] S. Paulotto, P. Baccarelli, F. Frezza, *et al.*, "A novel technique for open-stopband suppression in 1-D periodic printed leaky-wave antennas," *IEEE Transactions on Antennas and Propagation*, vol. 57, no. 7, pp. 1894–1906, 2009.

[12] N. Yang, C. Caloz, and K. Wu, "Full-space scanning periodic phase-reversal leaky-wave antenna," *IEEE Transactions on Microwave Theory and Techniques*, vol. 58, no. 10, pp. 2619–2632, 2010.

[13] S. Otto, Z. C. Chen, A. Al-Bassam, *et al.*, "Circular polarization of periodic leaky-wave antennas with axial asymmetry: Theoretical proof and experimental demonstration," *IEEE Transactions on Antennas and Propagation*, vol. 62, no. 4, pp. 1817–1829, 2014.

[14] S. Otto, A. Al-Bassam, A. Rennings, *et al.*, "Transversal asymmetry in periodic leaky-wave antennas for Bloch impedance and radiation efficiency equalization through broadside," *IEEE Transactions on Antennas and Propagation*, vol. 62, no. 10, pp. 5037–5054, 2014.

[15] W. L. Zhou, J. H. Liu, and Y. L. Long, "Investigation of shorting vias for suppressing the open stopband in an SIW periodic leaky-wave structure," *IEEE Transactions on Microwave Theory and Techniques*, vol. 66, no. 6, pp. 2936–2945, 2018.

[16] Y. L. Lyu, F. Y. Meng, G. H. Yang, *et al.*, "Leaky-wave antenna with alternately loaded complementary radiation elements," *IEEE Antennas and Wireless Propagation Letters*, vol. 17, no. 4, pp. 679–683, 2018.

[17] J. H. Liu, W. L. Zhou, and Y. L. Long, "A simple technique for open-stopband suppression in periodic leaky-wave antennas using two nonidentical elements per unit cell," *IEEE Transactions on Antennas and Propagation*, vol. 66, no. 6, pp. 2741–2751, 2018.

[18] H. Jiang, K. W. Xu, Q. F. Zhang, *et al.*, "Backward-to-forward wide-angle fast beam-scanning leaky-wave antenna with consistent gain," *IEEE Transactions on Antennas and Propagation*, vol. 69, no. 5, pp. 2987–2992, 2021.

[19] H. H. Wang, S. Sun, and X. H. Xue, "A periodic meandering microstrip line leaky-wave antenna with consistent gain and wide-angle beam scanning," *International Journal of RF and Microwave Computer-Aided Engineering*, vol. 32, no. 7, article no. e23162, 2022.

[20] H. H. Wang, S. Sun, and X. H. Xue, "A periodic CPW leaky-wave antenna with enhanced gain and broadside radiation," *IEEE Antennas and Wireless Propagation Letters*, vol. 21, no. 4, pp. 676–680, 2022.

[21] M. A. Antoniades and G. V. Eleftheriades, "A CPS leaky-wave antenna with reduced beam squinting using NRI-TL metamaterials," *IEEE Transactions on Antennas and Propagation*, vol. 56, no. 3, pp. 708–721, 2008.

[22] Y. D. Dong and T. Itoh, "Composite right/left-handed substrate integrated waveguide and half mode substrate integrat-

ed waveguide leaky-wave structures," *IEEE Transactions on Antennas and Propagation*, vol. 59, no. 3, pp. 767–775, 2011.
[23] G. Zamora, S. Zuffanelli, F. Paredes, *et al.*, "Fundamental-mode leaky-wave antenna (LWA) using slotline and split-ring-resonator (SRR)-based metamaterials," *IEEE Antennas and Wireless Propagation Letters*, vol. 12 pp. 1424–1427, 2013.
[24] A. Mehdipour and G. V. Eleftheriades, "Leaky-wave antennas using negative-refractive-index transmission-line metamaterial supercells," *IEEE Transactions on Antennas and Propagation*, vol. 62, no. 8, pp. 3929–3942, 2014.
[25] D. K. Karmokar, Y. J. Guo, S. L. Chen, *et al.*, "Composite right/left-handed leaky-wave antennas for wide-angle beam scanning with flexibly chosen frequency range," *IEEE Transactions on Antennas and Propagation*, vol. 68, no. 1, pp. 100–110, 2020.
[26] D. J. Wei, J. Y. Li, J. J. Yang, *et al.*, "Wide-scanning-angle leaky-wave array antenna based on microstrip SSPPs-TL," *IEEE Antennas and Wireless Propagation Letters*, vol. 17, no. 8, pp. 1566–1570, 2018.
[27] S. D. Xu, D. F. Guan, Q. F. Zhang, *et al.*, "A wide-angle narrowband leaky-wave antenna based on substrate integrated waveguide-spoof surface Plasmon polariton structure," *IEEE Antennas and Wireless Propagation Letters*, vol. 18, no. 7, pp. 1386–1389, 2019.
[28] D. K. Karmokar, S. L. Chen, T. S. Bird, *et al.*, "Single-layer multi-via loaded CRLH leaky-wave antennas for wide-angle beam scanning with consistent gain," *IEEE Antennas and Wireless Propagation Letters*, vol. 18, no. 2, pp. 313–317, 2019.
[29] D. K. Karmokar, S. L. Chen, D. Thalakotuna, P. Y. Qin, *et al.*, "Continuous backward-to-forward scanning 1-D slot-array leaky-wave antenna with improved gain," *IEEE Antennas and Wireless Propagation Letters*, vol. 19, no. 1, pp. 89–93, 2020.
[30] G. Zhang, Q. F. Zhang, Y. F. Chen, *et al.*, "High-scanning-rate and wide-angle leaky-wave antennas based on glide-symmetry Goubau line," *IEEE Transactions on Antennas and Propagation*, vol. 68, no. 4, pp. 2531–2540, 2020.
[31] P. F. Zhang, L. Zhu, and S. Sun, "Microstrip-line EH_1/EH_2-mode leaky-wave antennas with backward-to-forward scanning," *IEEE Antennas and Wireless Propagation Letters*, vol. 19, no. 12, pp. 2363–2367, 2020.
[32] Y. J. Chi and F. C. Chen, "CRLH leaky wave antenna based on ACPS technology with 180° horizontal plane scanning capability," *IEEE Transactions on Antennas and Propagation*, vol. 61, no. 2, pp. 571–577, 2013.
[33] R. Henry and M. Okoniewski, "A broadside-scanning half-mode substrate integrated waveguide periodic leaky-wave antenna," *IEEE Antennas and Wireless Propagation Letters*, vol. 13, pp. 1429–1432, 2014.
[34] R. Henry and M. Okoniewski, "A broadside scanning substrate integrated waveguide periodic phase-reversal leaky-wave antenna," *IEEE Antennas and Wireless Propagation Letters*, vol. 15, pp. 602–605, 2016.
[35] G. S. Kong, H. F. Ma, B. G. Cai, *et al.*, "Continuous leaky-wave scanning using periodically modulated spoof plasmonic waveguide," *Scientific Reports*, vol. 6, no. 1, article no. 29600, 2016.
[36] C. A. Balanis, *Antenna Theory: Analysis and Design*. 4th ed., Wiley, Hoboken, NJ, USA, 2015.
[37] Y. S. Pan, Y. Cheng, and Y. D. Dong, "Dual-polarized directive ultrawideband antenna integrated with horn and Vivaldi array," *IEEE Antennas and Wireless Propagation Letters*, vol. 20, no. 1, pp. 48–52, 2021.

Henghui WANG was born in Shandong Province, China, in 1995. He received the B.E. degree in electronic and information engineering from Hefei University of Technology, Hefei, China, in 2018. He is currently pursuing the Ph.D. degree in electronic science and technology with University of Electronic Science and Technology of China, Chengdu, China. His research interests include leaky-wave antennas, periodic structures, and calibration technology.
(Email: henghui_wang@126.com)

Peiyao CHEN was born in Anhui Province, China, in 1996. He received the B.E. and M.E. degrees from University of Electronic Science and Technology of China, Chengdu, China, in 2018 and 2021, respectively. He is currently pursuing the Ph.D. degree in electronic science and technology with University of Electronic Science and Technology of China, Chengdu, China. His research interests include planer leaky-wave antennas and filter synthesis.
(Email: peiyao-chen@outlook.com)

Sheng SUN was born in Shaanxi Province, China, in 1980. He received the B.E. degree in information engineering from Xi'an Jiaotong University, Xi'an, China, in 2001, and the Ph.D. degree in electrical and electronic engineering from Nanyang Technological University (NTU), Singapore, in 2006. From 2005 to 2006, he was with the Institute of Microelectronics, Singapore. From 2006 to 2008, he was a Post-Doctoral Research Fellow with NTU. From 2008 to 2010, he was a Humboldt Research Fellow with the Institute of Microwave Techniques, University of Ulm, Ulm, Germany. From 2010 to 2015, he was a Research Assistant Professor with The University of Hong Kong, Hong Kong, China. Since 2015, he has been a Full Professor with University of Electronic Science and Technology of China, Chengdu, China. He has authored or coauthored one book and two book chapters, and over 190 journal and conference publications. His current research interests include electromagnetic theory, computational electromagnetics, multiphysics, numerical modeling of planar circuits and antennas, microwave passive and active devices, and microwave and millimeter-wave communication systems. Prof. Sun was a recipient of the International Symposium on Antennas and Propagation (ISAP) Young Scientist Travel Grant, Japan, in 2004; the Hildegard Maier Research Fellowship of the Alexander Von Humboldt Foundation, Germany, in 2008; the Outstanding Reviewer Award of *IEEE Microwave and Wireless Components Letters* in 2010; and the General Assembly Young Scientists Award from the International Union of Radio Science in 2014. From 2010 to 2014, he was as an Associate Editor of *IEICE Transactions on Electronics*. He also serves as an Associate Editor for *IEEE Microwave and Wireless Components Letters*, *Electronics Letters* (IET), and the *International Journal of RF and Microwave Computer Aided Engineering*.
(Email: sunsheng@uestc.edu.cn)